VERSITA

Fractional Calculus & Applied Analysis

An International Journal for Theory and Applications

VOLUME 16, NUMBER 3 (2013)

(Print) ISSN 1311-0454
(Electronic) ISSN 1314-2224

SURVEY PAPER

EFFECTS OF THE TEMPERATURE VARIATION ON THE BEHAVIOR OF THE FIRST ORDER CRONE SYSTEM REALIZED IN THE ELECTRICAL DOMAIN

Roy Abi Zeid Daou [1], Xavier Moreau [2], Clovis Francis [3]

Abstract

This paper presents the effects of the temperature variation on the fractional order system of first kind realized in the electrical domain. The temperature variation, which is one of the parametric uncertainties which encounters the system's behaviour, alters the values of the resistive and capacitive (RC) components used for the realization of this fractional system. The experimental results show that the system behaviour remains unchanged. Hence, the main objective of this work is to study analytically if the recursive factors, used to calculate the resistances and capacitance on one hand, and used to determine the poles and zeros on the other hand, are still valid and thus, the recursion is conserved. The results found show that the system is not affected by the temperature variation and the system is still robust to such uncertainties.

Key Words and Phrases: CRONE controller, parametric uncertainties, components tolerance, electrical test bench, system dynamics, fractional behaviour

MSC 2010: 93B51, 93D09, 93C80, 94C05; 26A33

pp. 520–537 , DOI: 10.2478/s13540-013-0034-7

1. Introduction

The idea of the fractional calculus seems to be originated at the end of the XVII century by letters exchanged between Leibniz and L'Hospital, see e.g. in [6], [13]. Since then, many mathematicians and physicians work on this new concept from a mathematical and applications points of view. The most important classical contributions to this field as theory came from Riemann and Liouville [15]. In opposite, the applications of this concept in the physical domain were delayed almost by three centuries. For example, one of the first such contributions was proposed by Oustaloup in 1975 when he introduced the control of laser by a regulator of order 3/2, [16].

The fractional differentiation is used today as an useful tool in different application areas, as the hydropneumatic suspension [2], [22], the diffusive interface problems [24], the control of dynamic systems [4], [5], [18], [26], the image processing techniques [7], the identification of biological phenomena [8], [23], the electrical domain [9], [20], the electromagnetic field [19], the viscoelastic interface, [25] and much more. A realization of fractional order systems was proposed by Oustaloup [17] in the late 90's, using resistive and capacitive components. Different arrangements of RC cells were introduced and several methods to realize fractional order systems were proposed depending on the RC network in use, see e.g. Levron et al. [11]. However, the synthesis method used to calculate the band-limited fractional integrator is unique and independent of the realization process.

The procedure used in order to realize a fractional order system is divided into five steps, see [1], [14]. First, the user defines the required specifications of the system, then he sets the four high level parameters (which are sufficient to define the fractional order system). These parameters are the low transitional frequency ω_b, the high transitional frequency ω_h, the derivation order n, and the number N of cells to be used. The third step requires calculating the two recursive parameters α and η. The fourth step enables the computation of the N poles and the N zeros of the system. At the end, the last part defines the RC network in use and calculates the values of the resistive and the capacitive components.

Thus, the first step is to build the fractional order system in the electrical domain. Then, the next step relies on varying the temperature of this test bench and measuring its output. The experimental results shown are generalized theoretically in the last step. To do so, we will go from the realization phase to reach the recursive parameters values in order to find whether these values are maintained or they are influenced by the components variations due to the temperature alteration.

This paper is organized as follow: in Section **2**, a background study of the fractional systems is displayed. In Section **3**, the fractional order system of first kind in the electrical domain is realized. Section **4** presents the implementation results of the test bench when varying the temperature and the variable resistance R_v. Section **5** shows the relations derived from the uncertainties caused by the temperature variation and the variable resistance. At the end, the last section presents a conclusion and some future work.

2. Background

This part presents a background study of fractional derivation systems and the way to synthesize and realize the system. At the end of this section, the values of the resistive and capacitive components that may be used in the implementation of the test bench are introduced.

We consider the fundamental linear fractional differential equation of the first kind as defined in [10]:

$$\omega_u^{-n} \, {}_0d_t^n \, y(t) \; + \; y(t) \; = \; u(t), \tag{2.1}$$

where $n \in [1\ ,\ 2]$, $\omega_u \in \Re^{*+}$ and the fractional differential operator ${}_0d_t^n \, y(t)$ is meant (as in [12]), as the Riemann-Liouville fractional derivative (see e.g. [21]):

$${}_0d_t^n \, y(t) = \left(\frac{d}{dt}\right)^{\eta} {}_0I_t^{\eta-n} \, y(t), \quad \text{with integer } \eta \text{ so that } \eta - 1 < n \leq \eta, \tag{2.2}$$

and with the Riemann-Liouville integral of fractional order $n > 0$ defined as

$${}_0I_t^n \, y(t) = \frac{1}{\Gamma(n)} \int_0^t y(\tau)(t-\tau)^{n-1} d\tau.$$

The transfer function $H(s)$ associated to the fractional differential equation (2.1) is given by

$$H(s) \; = \; \frac{Y(s)}{U(s)} = \frac{1}{1 \; + \; \left(\frac{s}{\omega_u}\right)^n} \tag{2.3}$$

and can be interpreted as the transfer function of a unity feedback closed loop system with an open-loop transfer function $\beta(s)$ given by:

$$\beta(s) \; = \; \left(\frac{\omega_u}{s}\right)^n. \tag{2.4}$$

So, the fractional open-loop transfer function (relation (2.4)) becomes a limited-bandwidth fractional open-loop transfer function $L(s)$ given by:

$$L(s) \; = \; \frac{K}{s^2} \left(\frac{1 + \frac{s}{\omega_b}}{1 + \frac{s}{\omega_h}}\right)^m, \tag{2.5}$$

where m varies between 0 and 1.

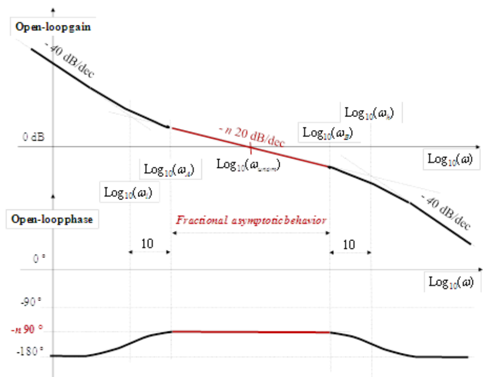

Fig. 2.1: Open-loop Bode diagrams [17]

Hence, to determine the fractional asymptotic behavior within the frequency range $[\omega_A, \omega_B]$ (Fig. 2.1), a practical rule leads to choose

$$\begin{cases} \omega_b &= \omega_A/10 \\ \omega_h &= 10\,\omega_B \end{cases} \quad \Rightarrow \quad a = \frac{\omega_h}{\omega_b} = 100\ \frac{\omega_B}{\omega_A}. \tag{2.6}$$

By taking ω_b and ω_h geometrically distributed around ω_{unom},

$$\sqrt{\omega_b\ \omega_h} = \omega_{unom}, \tag{2.7}$$

and by taking into account the ratio a defined by relation (2.7), ω_b and ω_h are given by:

$$\begin{cases} \sqrt{\omega_b\ \omega_h} = \omega_{unom} \\ a\ =\ \frac{\omega_h}{\omega_b} \end{cases} \quad \Rightarrow \quad \begin{cases} \omega_b &= \omega_{unom}/\sqrt{a} \\ \omega_h &= \omega_{unom}\ \sqrt{a} \end{cases}, \tag{2.8}$$

the fractional order system is well defined and calculated.

In order to synthesize and realize the fractional order integrator presented in equation (2.4), the rational form of this integrator is used [17]. This form consists on having a band-limited integrator defined by a number of poles and zeros as shown below:

$$I_N(s) = \frac{D_0}{s} \prod_{i=1}^{N} \left(\frac{1 + \frac{s}{\omega_i^{'}}}{1 + \frac{s}{\omega_i}} \right), \tag{2.9}$$

where N represents the number of RC cells, D_0 allows to have a unit gain for the central frequency ω_u and ω_i and $\omega_i^{'}$ represent the poles and the zeros of the system:

$$\begin{aligned} &\alpha\eta = \left(\frac{\omega_h}{\omega_b}\right)^{1/N}, \quad \eta = (\alpha\eta)^{1-m}, \quad \alpha = (\alpha\eta)^{m}, \\ &\omega_1^{'} = \sqrt{n} \times \omega_b \quad, \quad \omega_N = \frac{1}{\sqrt{n}}\omega_h \;, \quad \frac{\omega_i}{\omega_i^{'}} = \alpha > 1, \\ &\frac{\omega_{i+1}^{'}}{\omega_i} = \eta > 1 \quad \text{and} \quad \frac{\omega_{i+1}^{'}}{\omega_i^{'}} = \frac{\omega_{i+1}}{\omega_i} = \alpha\eta > 1. \end{aligned} \tag{2.10}$$

Then, the poles and the zeros are calculated using the remaining relations of (2.10). Once determined, we can find that each pole is located between two zeros and each zero is located between two poles. In other words, there are not two or more consecutive poles or zeros.

The poles and the zeros being defined, the last step is to choose the RC network in use and to calculate the values of the resistors and the capacitors. Two different arrangements were studied in previous works [3]; however, for the electrical application, only the parallel arrangement of RC cells in series is treated. The values of the resistors and the capacitors are calculated using the decomposition in simple fraction method.

As an example, we will present in the last part of this section a numerical illustration. The values found here will be used in the electrical test bench that is discussed in the next section. To start, the user specifications are as follow:

$$\left\{\begin{array}{l} \omega_{u_{nom}} = 600\ rad/s \quad ; \quad M_\Phi = 45° \quad ; \quad N = 5 \\ m \ = \ M_\Phi/90° \quad \Rightarrow \quad m \ = \ 0.5 \\ \omega_b \ = \ \omega_{u_{nom}}/20 \quad \Rightarrow \quad \omega_b \ = \ 30\ rad/s \\ \omega_h \ = \ 20\ \omega_{u_{nom}} \quad \Rightarrow \quad \omega_h \ = \ 12000\ rad/s \end{array}\right. . \tag{2.11}$$

So, the four high-level parameters used in the fractional integrator (relation (2.11)) are determined and the next step is to represent this fractional integrator using the rational model. To do this, we have chosen to use 5 RC cells. Knowing that the integrator order is 0.5, the recursive factors α and η are given by:

$$\alpha = \left(\frac{\omega_h}{\omega_b}\right)^{\left(\frac{m}{N}\right)} = 1.820 \tag{2.12}$$

and

$$\eta = \left(\frac{\omega_h}{\omega_b}\right)^{\left(\frac{1-m}{N}\right)} = 1.820. \tag{2.13}$$

Hence the values of the five poles and the five zeros lead to the choice of:

$$\left\{\begin{array}{l} \omega_1^{'} = 40.47\ rad/s \\ \omega_2^{'} = 134.66\ rad/s \\ \omega_3^{'} = 450.36\ rad/s \\ \omega_4^{'} = 1500.02\ rad/s \\ \omega_5^{'} = 4985.08\ rad/s \end{array}\right. \text{ and } \left\{\begin{array}{l} \omega_1 = 73.69\ rad/s \\ \omega_2 = 246.86\ rad/s \\ \omega_3 = 823.00\ rad/s \\ \omega_4 = 2736.51\ rad/s \\ \omega_5 = 9086.11\ rad/s \end{array}\right. . \tag{2.14}$$

The last step is to calculate the values of the resistances and the capacitors in order to realize this fractional controller. The values of these components are as follow:

$$\left\{\begin{array}{l} \mathrm{R}_1 = 289.72 \times 10^3\ \Omega \\ \mathrm{R}_2 = 244.25 \times 10^3\ \Omega \\ \mathrm{R}_3 = 148.58 \times 10^3\ \Omega \\ \mathrm{R}_4 = 87.365 \times 10^3\ \Omega \\ \mathrm{R}_5 = 57.730 \times 10^3\ \Omega \end{array}\right. \text{ and } \left\{\begin{array}{l} C_0 = 7.453 \times 10^{-9}\mathrm{F} \\ C_1 = 85.26 \times 10^{-9}\mathrm{F} \\ C_2 = 30.40 \times 10^{-9}\mathrm{F} \\ C_3 = 14.94 \times 10^{-9}\mathrm{F} \\ C_4 = 7.630 \times 10^{-9}\mathrm{F} \\ C_5 = 3.474 \times 10^{-9}\mathrm{F} \end{array}\right. . \qquad (2.15)$$

3. Electrical test bench

Fig. 3.1 represents the electrical circuit that handles the fractional order integrator using the parallel arrangement of RC cells in series. This circuit is divided into three parts:

- Differential amplifier with a unit gain;
- Fractional order integrator based on the parallel arrangement of RC cells in series;
- First order integrator.

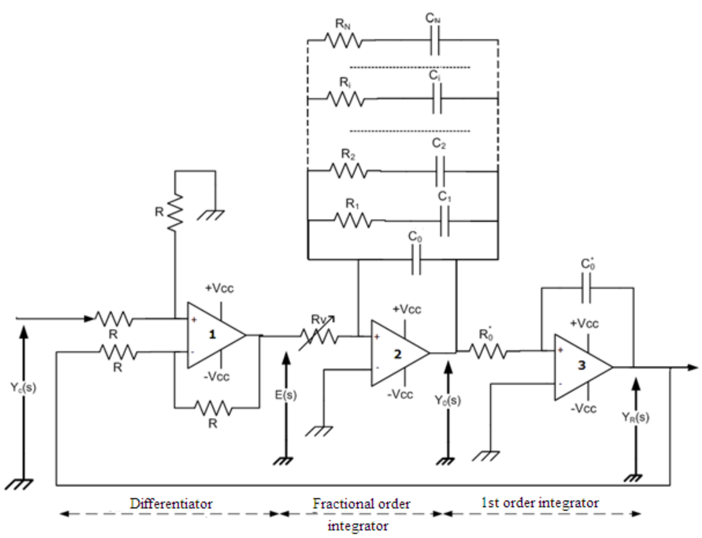

Fig. 3.1: Electrical circuit of the test bench

In more details, as both resistances R at the input of the operational amplifier of the first stage are identical, the Laplace transform of the output of this stage $E(s)$ is equal to the difference between the input of the circuit $Y_c(s)$ and the output of the feedback $Y_R(s)$, hence:

$$E(s) = Y_c(s) - Y_R(s). \qquad (3.1)$$

For the second stage which constitutes the band-limited fractional order integrator, the relation that links the output $Y_0(s)$ to the input $E(s)$ is given by:

$$Y_0(s) = -\frac{Z_f(s)}{R_v} \times E(s), \tag{3.2}$$

where $Z_f(s)$ represents the input impedance of the parallel arrangement of RC cells in series which has the following expression [9]:

$$Z_f(s) = \frac{1}{C_0 s + \sum\limits_{i=1}^{N} \frac{C_i s}{1+R_i C_i s}}. \tag{3.3}$$

Note that this impedance is an approximation of the band-limited fractional order integrator $I_N(s)$ shown in relation (2.9).

The relation between the input $Y_0(s)$ and the output $Y_R(s)$ of the third stage, which represent a first order integrator, can be represented as follows:

$$Y_R\,(s) \;=\; -\,\frac{1}{R_0^*\;C_0^*\;s}\;Y_0\,(s)\,. \tag{3.4}$$

Finally, the open loop transfer function *L(s)* is as follows:

$$L\,(s) \;=\; \frac{B_0}{s^2}\left(\frac{1+\frac{s}{\omega_b}}{1+\frac{s}{\omega_h}}\right)^m, \tag{3.5}$$

where B_0 is a constant defined by:

$$B_0 \;=\; \frac{D_0}{R_v\;R_0^*\;C_0^*}\,. \tag{3.6}$$

Note that:

- the variable resistance R_v is used to analyze the stability degree robustness of the system when varying the unit gain frequency ω_u;

- the variable resistance value is chosen with a particular attention as the unit gain frequency in open loop ω_u must be always in the phase constancy region and referring to the previously shown relations, B_0 and ω_u depend on the value of R_v;

- the resistance R_0^* and the capacitor C_0^* are chosen in such a way that the inverse of the integration time constant $\tau_i = R_0^* \times C_0^*$ is equal to the unit gain frequency in open loop ω_u for the nominal parametric state of the fractional system, to know:

$$\omega_{u_{nom}} \;=\; 1/\,(R_0^*\;C_0^*)\,. \tag{3.7}$$

When implementing the fractional order system, some alterations of the resistive and capacitive values (found in relation 2.15) occur. The main rule used in the implementation process is to used at maximum three resistances or three capacitors, placed in series or in parallel, to get the closest value possible to the optimal one found by calculation. Thus, the real values of the resistors and the capacitors are the following:

$$\begin{cases} \mathrm{R}_1 = 300\ k\Omega \\ \mathrm{R}_2 = 250\ k\Omega \\ \mathrm{R}_3 = 150\ k\Omega \\ \mathrm{R}_4 = 90\ k\Omega \\ \mathrm{R}_5 = 62\ k\Omega \end{cases} \quad \text{and} \quad \begin{cases} C_0 = 8\ nF \\ C_1 = 85\ nF \\ C_2 = 30\ nF \\ C_3 = 15\ nF \\ C_4 = 7\ nF \\ C_5 = 3.3\ nF \end{cases}. \tag{3.8}$$

Furthermore, the values of the remaining components of the test bench are as follow:

$$\begin{cases} C_0^* &= 1\ \mu\mathrm{F} \\ R_v &= 50\ \mathrm{k}\Omega \\ D_0 &= 67.08\ \times\ 10^5 \\ R_0^* &= 1.67\ \mathrm{k}\Omega \end{cases}. \tag{3.9}$$

Fig. 3.2 represents a comparison between the response of the system when using the ideal values of the resistances and the capacitors (in blue) - relation (2.15) - and the real values (in green) - relation (3.8) - used in the implementation phase. In more details, Fig. 3.2(a) shows the system response of the open loop in the Bode diagrams when using the ideal and the real values of the resistances and the capacitors whereas Fig. 3.2(b) presents the system's step response when using these two sets of components values. The results show that the behavior of the system is not affected when using the ideal values of the resistances and the capacitors and their approximations.

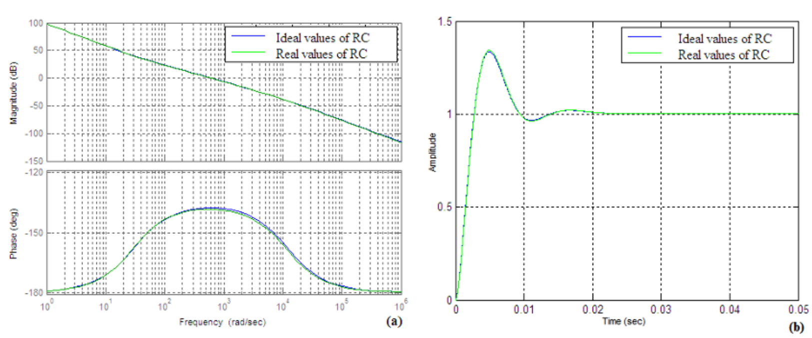

Fig. 3.2: Behavior of the fractional order system when using the ideal RC values (relation 2.15) and the implemented ones (relation 3.8). In more details, (a) represents Bode diagrams in open loop and (b) shows the step response of the system

4. Temperature uncertainties measurements

In this part, the test bench results are presented. This electronic circuit has been implemented using the values of the electrical resistors and capacitors shown in relation (3.8).

The two main parameters have been modified during the tests: the temperature and the variable resistance R_v. The first parameter is modified in order to see whether the phase constancy remains constant even with the temperature alteration whereas the second parameter is used to study the robustness of the system.

Hence, this section is divided in two parts: in the first one, some numerical simulations are shown especially in frequency domain whereas, in the second part, the results obtained on the oscilloscope are presented.

4.1. Numerical simulation

The first simulation shows the robustness of the system when varying the value of the variable resistance R_v. The values of this resistance were chosen in such a way that, even for the minimum and maximum values, the new values of the unit gain frequency ω_u remain in the phase constancy zone already defined to be between ω_b and ω_h. So, the two extreme values of the variable resistance R_v, notably 18kΩ and 140kΩ, correspond to a unit gain frequency of about 1200rad/sec and 300rad/sec, respectively.

Thus, Fig. 4.1 represents the behavior of the system for the three different values of R_v. In more details, Fig. 4.1(a) represents the Bode diagrams of the band limited fractional order integrator, Fig. 4.1(b) shows the behavior of the open loop system in the Bode diagrams, Fig. 4.1(c) presents the Black-Nichols diagram in open loop and Fig. 4.1(d) correspond to the closed loop step response. Note that, for all figures, the outputs in solid blue represent the response of the system when using the nominal value of the variable resistance ($R_v = 50\text{k}\Omega$) whereas the dashed green outputs are related to the minimal resistance value ($R_v = 18\text{k}\Omega$) and the dashed-dotted red lines represent the response of the system for the maximal resistance value ($R_v = 140\text{k}\Omega$).

These results prove, once more, that the stability degree robustness is an important property of the fractional order systems independently on the domain of application.

The objective of the second simulation was to study the stability degree robustness of the system when varying the resistance R_v and the ambient temperature. Hence, Fig. 4.2 and Fig. 4.3 show the time domain responses for the three different temperature values when applying a triangular impulse (Fig. 4.2) and a period rectangle (Fig. 4.3). The temperature values are chosen to be $0°C$, $22°C$ and $40°C$. Note that the values of the resistances and the capacitors used in these simulations are the ones found when these components are subject to the predefined temperature values.

The results found show that stability degree of the fractional systems of first kind is insensible to resistance and temperature variation.

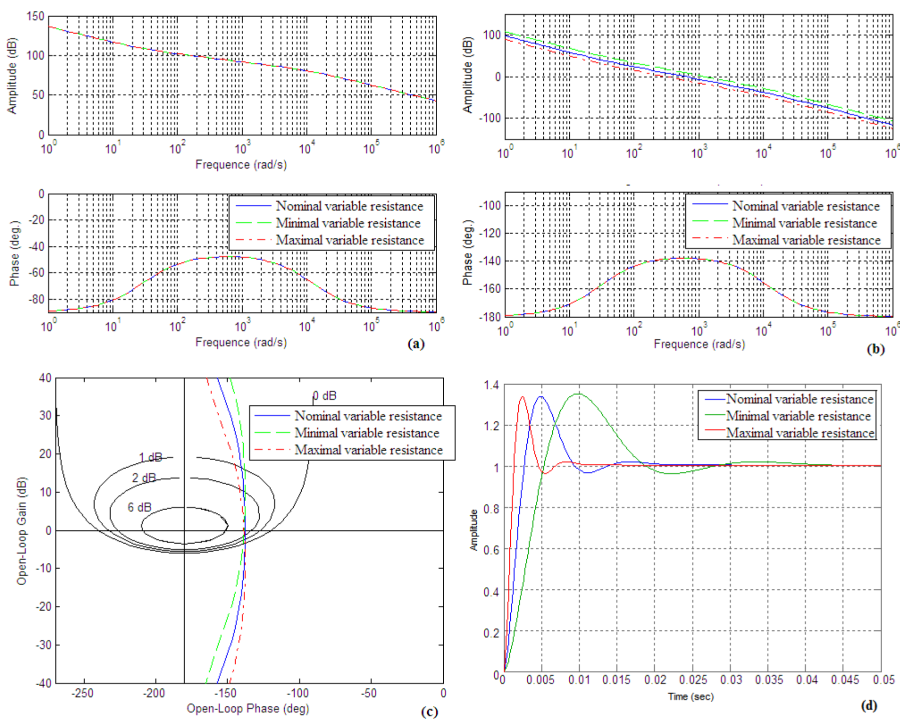

Fig. 4.1: Study of the stability degree robustness with respect to the variation of R_v: (a) Bode diagrams of the band limited fractional order integrator, (b) open loop system in the Bode diagrams,(c) Black-Nichols diagram in open loop and (d) closed loop step response

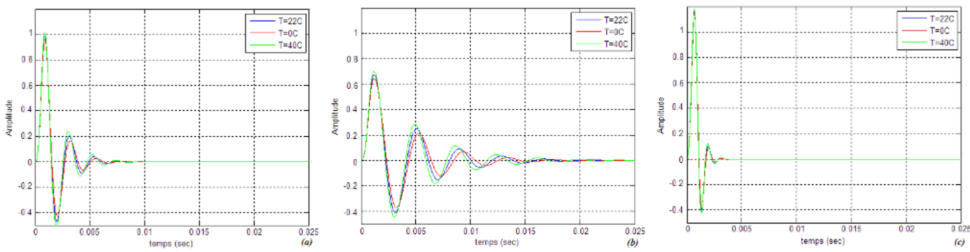

Fig. 4.2: Simulation results when applying a triangular impulse for the three different temperature values and for: (a) Rv = 50 KΩ (b) Rv = 140 KΩ and (c) Rv = 18 KΩ

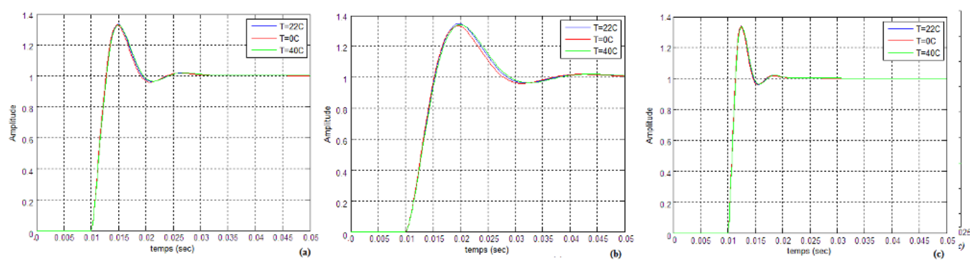

Fig. 4.3: Simulation results when applying a periodic rectangular input for the three different temperature values and for: (a) Rv = 50 KΩ (b) Rv = 140 KΩ and (c) Rv = 18 KΩ

4.2. Implementation results

In this second part, we present the implementation results of the test bench subject to temperature variations. So, we introduce at the beginning some photos of the test bench. Then, the outputs of the oscilloscope are recovered.

Hence, Fig. 4.4 represents the implemented test bench with the measurement instruments used to stimulate and to retrieve the output of this system for different temperature values. Thus, Fig. 4.4(a) represents the test bench placed in the ambient temperature, which varies between $19°C$ and $23°C$, Fig. 4.4(b) represents the test bench placed in a temperature of about $0°C$ and, finally, Fig. 4.4(c) shows the electrical bench subject to $40°C$. To remember that, even during temperature variation, the variable resistance R_v is also altered in order to study the robustness of the system.

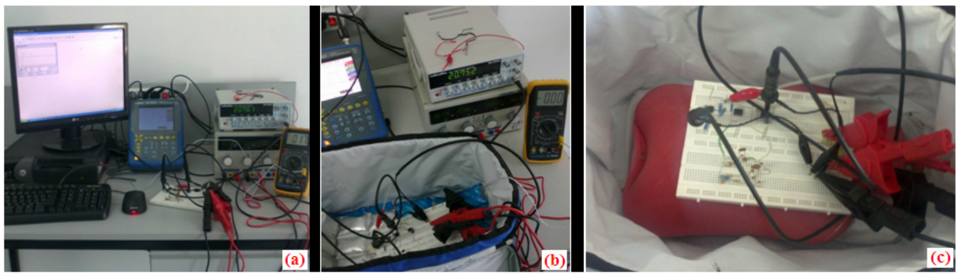

Fig. 4.4: Implementation of the electrical test bench and measurement of the output for different temperature values

Fig. 4.5 represents the output of the system for the three different temperatures and for the three values of R_v. In more details, Fig. 4.5(a) shows the system response for the three temperatures when R_v values is equal to 18KΩ, whereas Fig. 4.5(b) shows the system response for the variable resistance nominal value ($R_v = 50$KΩ) and finally, Fig. 4.5(c) shows the system output for the maximal value of the variable resistance ($R_v = 140$KΩ). Note that, in the three subfigures, the output in blue represents the system's response when it is under $40°C$, the one in green shows the system behaviour when it is subject to $22°C$ and, finally, the output in brown shows the system response when it is maintained around $0°C$.

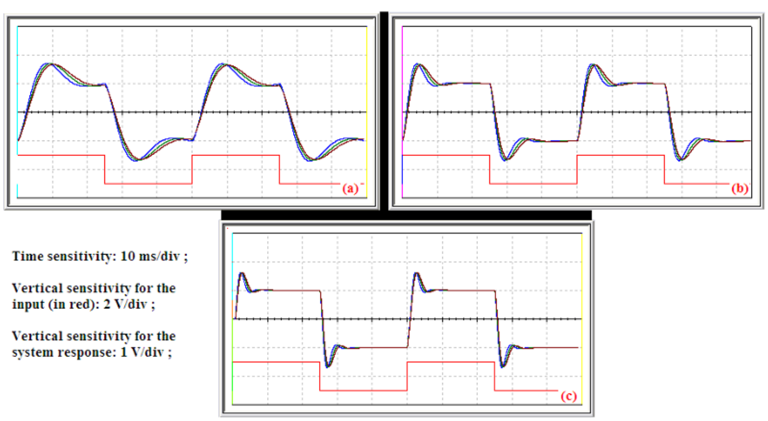

Fig. 4.5: Output of the test bench for different temperature values and for different values of the variable resistance R_v. In more details, the system output for (a) $R_v = 18$KΩ, (b) $R_v = 50$KΩ and (c) $R_v = 140$KΩ are represented.

The three sub-figures show clearly that the system in use is robust toward temperature and variable resistance alterations. It is remarkable that the temperature variation do not modify the output of the system. Also, the variations in the variable resistance value modify only the response time of the system without introducing significant changes in the first overshoot value. These results lead to the fact that the CRONE system of first order is robust and it is not affected by the uncertainties related to temperature variation.

5. Theoretical analysis

In this part, we try to explain from a theoretical point of view the results shown in the previous section. So, the uncertainties related to the temperature variation are taken into consideration. Suppose that the real values of the resistances and the capacitors are now $\tilde{R}_i$ and $\tilde{C}_i$. The relations between these values and the ones found in the synthesis process are as follow:

$$\begin{cases} \tilde{R}_i \;=\; R_i \;+\; \Delta_a R_i = R_i(1+\Delta_m R_i) \\ \tilde{C}_i \;=\; C_i \;+\; \Delta_a C_i = C_i(1+\Delta_m C_i) \end{cases}, \tag{5.1}$$

where $\Delta_a R_i$ and $\Delta_a C_i$ represent the uncertainties using the additive method and $\Delta_m R_i$ and $\Delta_m C_i$ represent the uncertainties using the multiplicative method.

When realizing this fractional order system, the system's recursion was present through the following relation:

$$\begin{cases} \frac{R_i}{R_{i+1}} \;=\; \eta \\ \frac{C_i}{C_{i+1}} \;=\; \alpha \end{cases}, \tag{5.2}$$

where α and η are the two recursive factors.

Thus, the main objective of this part is to show if this recursion will still be valid after introducing the uncertainties on the resistive and capacitive values.

After introducing the uncertainties, relation (5.2) becomes:

$$\begin{cases} \frac{\tilde{R}_i}{\tilde{R}_{i+1}} \;=\; \frac{R_i}{R_{i+1}} \left(\frac{1+\Delta_m R_i}{1+\Delta_m R_{i+1}}\right) \;=\; \eta \left(\frac{1+\Delta_m R_i}{1+\Delta_m R_{i+1}}\right) \\ \frac{\tilde{C}_i}{\tilde{C}_{i+1}} \;=\; \frac{C_i}{C_{i+1}} \left(\frac{1+\Delta_m C_i}{1+\Delta_m C_{i+1}}\right) \;=\; \alpha \left(\frac{1+\Delta_m C_i}{1+\Delta_m C_{i+1}}\right) \end{cases}. \tag{5.3}$$

So, we will have two vectors α and η, each one consisting of N values, N being the number of cells constituting the fractional order system.

A *Hypothesis H1* is considered in this case:
If we assume that:

- the multiplicative uncertainties related to manufacturing variations are negligible toward the unit;

- all the RC network components are subjected to the same temperature variation values;

- all resistances, on one hand, and all capacitors, on the other hand, have the same sensitivity to temperature variation;

Then, the resulting uncertainties $\Delta_m R$ and $\Delta_m C$ are the same for all components R, on the one hand, and components C, on the other hand. This means that they no longer dependent on the rang i of the cell.

In this case, relation (5.3) can be rewritten as follows:

$$\left\{ \begin{array}{lcl} \frac{\tilde{R}_i}{\tilde{R}_{i+1}} & = & \frac{R_i}{R_{i+1}} \left(\frac{1+\Delta_m R}{1+\Delta_m R} \right) \\ \frac{\tilde{C}_i}{\tilde{C}_{i+1}} & = & \frac{C_i}{C_{i+1}} \left(\frac{1+\Delta_m C}{1+\Delta_m C} \right) \end{array} \right. . \tag{5.4}$$

It can even be simpler as shown below:

$$\left\{ \begin{array}{lclcl} \frac{\tilde{R}_i}{\tilde{R}_{i+1}} & = & \frac{R_i}{R_{i+1}} & = & \eta \\ \frac{\tilde{C}_i}{\tilde{C}_{i+1}} & = & \frac{C_i}{C_{i+1}} & = & \alpha \end{array} \right. \quad \text{as} \quad \left\{ \begin{array}{l} \Delta_m R << 1 \\ \Delta_m C << 1 \end{array} \right. . \tag{5.5}$$

Hence, relation (5.5) shows that the recursion of the electrical components is still present with the same factors α and η.

Let us check if this recursion is also maintained in the frequency domain. The three relations that represent the frequency parameters with respect to the resistive and capacitive components are the following:

$$\left\{ \begin{array}{lcl} D_0 & = & \frac{1}{\sum\limits_{i=0}^{N} C_i} \\ \omega_i^{'} & = & \frac{1}{R_i\, C_i} \\ \omega_i & = & \frac{1}{R_i\, C_{i+1}} \end{array} \right. . \tag{5.6}$$

The introduction of the uncertainties to the resistive and capacitive components leads to new relations of D_0, $\omega_i^{'}$ and ω_i. These relations are presented below:

$$\left\{ \begin{array}{l} \tilde{D}_0 = \frac{1}{\sum\limits_{i=0}^{N} (C_i + \Delta_a C_i)} = \frac{1}{\sum\limits_{i=0}^{N} C_i + \sum\limits_{i=0}^{N} \Delta_a C_i} = \frac{1}{\sum\limits_{i=0}^{N} C_i \left(1 + \frac{\sum\limits_{i=0}^{N} \Delta_a C_i}{\sum\limits_{i=0}^{N} C_i} \right)} \\ \tilde{\omega}_i^{'} = \frac{1}{R_i\, C_i}\, \frac{1}{(1+\Delta_m R_i)\, (1+\Delta_m C_i)} \\ \tilde{\omega}_i = \frac{1}{R_i\, C_{i+1}}\, \frac{1}{(1+\Delta_m R_i)\, (1+\Delta_m C_{i+1})} \end{array} \right. , \tag{5.7}$$

or, it can be written as follows:

$$\begin{cases} \tilde{D}_0 \; = \; D_0 \, \Delta D_0 \quad \text{with} \;\; \Delta D_0 = \left(1 + \dfrac{\sum\limits_{i=0}^{N} \Delta_a C_i}{\sum\limits_{i=0}^{N} C_i}\right)^{-1} \\ \tilde{\omega}_i^{'} \; = \; \omega_i^{'} \, \frac{1}{(1+\Delta_m R_i)\,(1+\Delta_m C_i)} \\ \tilde{\omega}_i \; = \; \omega_i \, \frac{1}{(1+\Delta_m R_i)\,(1+\Delta_m C_{i+1})} \end{cases} . \tag{5.8}$$

The ratio between the transient frequencies $\omega_i^{'}$ and ω_i, when taking into consideration the uncertainties of the resistive and capacitive components, is:

$$\begin{cases} \frac{\tilde{\omega}_i}{\tilde{\omega}_i^{'}} = \frac{\omega_i}{\omega_i^{'}} \; \frac{(1+\Delta_m R_i)\,(1+\Delta_m C_i)}{(1+\Delta_m R_i)\,(1+\Delta_m C_{i+1})} & = \; \alpha \; \frac{(1+\Delta_m C_i)}{(1+\Delta_m C_{i+1})} \\ \frac{\tilde{\omega}_{i+1}^{'}}{\tilde{\omega}_i} \; = \; \frac{\omega_{i+1}^{'}}{\omega_i} \; \frac{(1+\Delta_m R_i)\,(1+\Delta_m C_{i+1})}{(1+\Delta_m R_{i+1})\,(1+\Delta_m C_{i+1})} & = \; \eta \; \frac{(1+\Delta_m R_i)}{(1+\Delta_m R_{i+1})} \end{cases} . \tag{5.9}$$

Therefore, taking into account the conditions presented in the Hypothesis *H1*, to remember,

$$\begin{cases} \Delta_m R_i = \Delta_m R_{i+1} = ... = \Delta_m R_N = \Delta_m R \\ \Delta_m C_i = \Delta_m C_{i+1} = ... = \Delta_m C_N = \Delta_m C \\ \Delta_m R_i \; << \; 1 \quad ; \quad \Delta_m C_i \; << \; 1 \\ \sum\limits_{i=0}^{N} \Delta_a C_i \; << \; \sum\limits_{i=0}^{N} C_i \end{cases} , \tag{5.10}$$

relation (5.8) can be rewritten as following:

$$\begin{cases} \frac{\tilde{\omega}_i}{\tilde{\omega}_i^{'}} \; = \; \alpha \; \frac{(1+\Delta_m C)}{(1+\Delta_m C)} \\ \frac{\tilde{\omega}_{i+1}^{'}}{\tilde{\omega}_i} \; = \; \eta \; \frac{(1+\Delta_m R)}{(1+\Delta_m R)} \end{cases} . \tag{5.11}$$

Hence,

$$\begin{cases} \frac{\tilde{\omega}_i}{\tilde{\omega}_i^{'}} = \; \alpha \\ \frac{\tilde{\omega}_{i+1}^{'}}{\tilde{\omega}_i} \; = \; \eta \end{cases} . \tag{5.12}$$

Thus, taking into consideration the Hypothesis *H1*, the frequency recursion is conserved even if the resistive and capacitive components' values are subject to temperature variation.

6. Conclusion

In this paper, we have presented the CRONE system of first kind applied to the electrical domain. The test bench used to implement the parallel arrangement of RC cells in series is also presented and analyzed. The synthesis and realization processes are also presented briefly as they were treated in different previous works.

The results found show that the system output is not altered by the temperature variation and the output is almost independent of the external temperature for the values taken in consideration. This meets with the theoretical results found where it had been shown that the temperature do not affect the recursive parameters α and η.

As a future work, other uncertainties related to the electrical domain will be studied as the components tolerance and deformation. Also, this work can be extended to other engineering domains as the hydropneumatic suspension, the diffusive interfaces, etc.

References

[1] R. Abi Zeid Daou, C. Francis, X. Moreau, Synthesis and implementation of non-integer integrators using RLC devices. *International J. of Electronics* **96**, No 12 (2009), 1207–1223.

[2] R. Abi Zeid Daou, C. Francis, X. Moreau, Study of the inertial effect and the nonlinearities of the CRONE suspension based on the hydropneumatic technology. *Nonlinear Dynamics* (*An Intern. J. of Nonlinear Dynamics and Chaos in Engineering Systems*) **63**, No 1-2 (2010), 1–17.

[3] R. Abi Zeid Daou, C. Francis and X. Moreau, Free and forced modes responses of fractional operators based on non-identical RLC cells. *Intern. J. of Adaptive and Innovative Systems* **1**, No 3/4 (2010), 318–333.

[4] R. Abi Zeid Daou, X. Moreau, C. Francis, Control of hydro-electromechanical system using the generalized PID and the CRONE controllers. In: *18th World Congress of the Intern. Federation of Automatic Control* (*IFAC*), Milano, Italy, Aug. 18 - Sept. 2, 2011.

[5] A. Charef, N. Fergani, $PI^{\lambda}D^{mu}$ controller tuning for desired closed-loop response using impulse response, In: *4th IFAC Workshop on Fractional Differentiation and Applications*, Badajoz, Spain, October 2010.

[6] S. Das, *Functional Fractional Calculus.* Springer, 2nd Ed. (2011).

[7] M.O. Franz, B. Scholkopf, Implicit Wiener series for higher-order image analysis. In: *Advances in Neural Information Processing Systems* **17** (Eds: L.K. Saul, Y. Weiss, L. Bottou), MIT Press, Cambridge – MA, 465–472.

[8] C. Ionescu, K. Desager, R. De Keyser, Fractional order model parameters for the respiratory input impedance in healthy and in asthmatic children. *Computer Methods and Programs in Biomedicine* **101**, No 3 (March 2011), 315–323.

[9] I. Jesus, J. Tenreiro Machado, Development of fractional order capacitors based on electrolyte processes. *Nonlinear Dynam.* **56** (2009), 45–55.

[10] B.T. Krishna, Studies on fractional order differentiators and integrators: A survey. *Signal Processing* **91** (2011), 386–426.

[11] F. Levron, J. Sabatier, A. Oustaloup, L. Habsieger, From partial differential equations of propagative recursive systems to non integer differentiation. *Fract. Calc. Appl. Anal.* **2**, No 3 (1999), 245–264.

[12] C.F. Lorenzo, T.T. Hartley, Initialization of fractional differential equations: Background and theory. In: *Proc. of the ASME' 2007* (Las Vegas, Nevada – USA, Sept. 4-7, 2007), Paper # DETC2007-34810.

[13] K.S. Miller, B. Ross, *An Introduction to the Fractional Calculus and Fractional Differential Equations*. Wiley, New York (1993).

[14] X. Moreau, O. Altet, A. Oustaloup, Fractional differentiation: An example of phenomenological interpretation. Chapter in: *Fractional Differentiation and its Applications*, U-Books Edition (2005), 275–287.

[15] K.B. Oldham, J. Spanier, *The Fractional Calculus*. Academic Press, New York (1974).

[16] A. Oustaloup, Etude et réalisation d'un système d'asservissement d'ordre 3/2 de la fréquence d'un laser colorant continu. *PhD Thesis,* Univ. Bordeaux I – France (1975).

[17] A. Oustaloup, *La dérivation non entière: théorie, synthèse et applications*. Hermes (1995).

[18] A. Oustaloup, J. Sabatier, P. Lanusse, From fractal robustness to the CRONE control. *Fract. Calc. Appl. Anal.* **2**, No 1 (1999), 1–30.

[19] A. Oustaloup, V. Pommier, P. Lanusse, Design of fractional control using performance contours. Application to an electromechanical system. *Fract. Calc. Appl. Anal.* **6**, No 1 (2003), 1–24.

[20] A.A. Rousan, N.Y. Ayoub, A fractional LC-RC circuit. *Fract. Calc. Appl. Anal.* **9**, No 1 (2006), 33–42; at http://www.math.bas.bg/∼fcaa .

[21] S.G. Samko, A.A. Kilbas, O.I. Marichev, *Fractional Integrals and Derivatives: Theory and Applications*. Gordon and Breach, Amsterdam (1993).

[22] P. Serrier, X. Moreau, A. Oustaloup, Limited-bandwidth fractional differentiator: Synthesis and application in vibration isolation. Chapter in: *Advances in Fractional Calculus*, Springer (2007), 287–302.

[23] A. Sommacal, P. Melchior, J.-M. Cabelguen, A. Oustaloup, A.-J. Ijspeert, Fractional multi-models of the gastrocnemius frog muscle. *J. of Vibration and Control* **14**, No 9-10 (2008), 1415–1430.

[24] J.C. Trigeassou, N. Maamri, Initial conditions and initialization of linear fractional differential equations. *Signal Processing* **91**, No 3 (2011), 427–436.

[25] B. Stankovic, T.M. Atanackovic, On a model of viscoelastic rod. *Fract. Calc. Appl. Anal.* **4**, No 4 (2001), 501–522.

[26] B.M. Vinagre, I. Podlubny, A. Hernandez, V. Feliu, Some approximations of fractional order operators used in control theory and applications. *Fract. Calc. Appl. Anal.* **3**, No 3 (2000), 231–248.

[1] *Lebanese German University*
Fac. of Public Health, Biomedical Technologies Department
Sahel Alma – P.O. Box: 206, Jounieh, LEBANON

e-mail: r.abizeiddaou@lgu.edu.lb

Received: May 21, 2012

Revised: October 14, 2012

[2] *University of Bordeaux I*
Laboratory IMS, Department LAPS
33405 Talence, cedex, Bordeaux, FRANCE

e-mail: xavier.moreau@ims-bordeaux.fr

[3] *Lebanese University, Faculty of Engineering I*
Tripoli, LEBANON

e-mail: cfrancis@ul.edu.lb

Please cite to this paper as published in:

Fract. Calc. Appl. Anal., Vol. **16**, No 3 (2013), pp. 520–537;
DOI: 10.2478/s13540-013-0034-7